URTeC: 2796

Using Multidisciplinary Data Gathering to Evaluate eXtreme Limited Entry Completion Design and Improve Perforation Cluster Efficiency

Apiwat (Ohm) Lorwongngam*, Shawn Wright*, Stephanie Hari*, Erin Butler, Michael McKimmy, Jennifer Wolters, Craig Cipolla, Hess Corporation

This paper was prepared for presentation at the Unconventional Resources Technology Conference held in Austin, Texas, USA, 20-22 July 2020.

Abstract

Lateral targeting, well spacing, and completion design are three controllable variables of production for unconventional wells. Achieving the right balance between these variables results in wellbore configurations that minimize hydraulic fracture overlap, create enough fracture surface area to drain targeted reservoirs effectively, with minimal capital investment. Many operators have recently turned to eXtreme Limited Entry (XLE) Plug and Perf (P&P) as a method to increase the number of perforation clusters (i.e., fractures) while maintaining efficient proppant and fluid delivery. To achieve XLE, operators must vary perforation hole size, pump rate, and the number of holes to achieve higher perforation entry pressures. The planned result is high cluster efficiency, even in stages with a high number of clusters. By increasing clusters per stage and achieving high cluster efficiency, operators can effectively stimulate unconventional wells with fewer stages, thus reducing the amount of time and capital it takes to complete a well.

This paper presents a case study of the successful implementation of XLE with interdisciplinary evaluation and validation. The case study resulted in significant improvements and cost reductions in the completion designs. XLE was implemented on two batches in Williston Basin, ND. Both batches consist of Three Forks (TF) and Middle Bakken (MB) wells in a wine-rack pattern. The number of clusters per stage was varied from 6 to 15 to test variable cluster efficiency using XLE. Carbon fiber rod deployed fiber optics data (DAS and DTS), downhole camera surveillance, step-down tests, and radioactive (RA) proppant tracers were collected and integrated with the geological targeting data and daily fluid production rates for three of the wells (1 MB, 2 TF) to validate the efficiency of high cluster XLE stages.

Pump pressures and step-down tests confirm that the high perforation entry pressures required for XLE were achieved for all stages. RA tracer and DAS/DTS data indicate that 85–95% cluster efficiency is achieved using XLE, even in the higher cluster count stages. High cluster efficiency appears to be independent of the geologic target in both MB and TF wells. However, a slightly lower efficiency was achieved in stages that were completed within the TF interbedded unit. A minor heel-to-toe bias was observed in the DAS/DTS data. This was confirmed by the downhole camera data showing more perforation erosion in heel-ward perforations compared to toe-ward perforations.

The use of multidisciplinary data gathering and integration resulted in significant improvements to completion designs, confirming that XLE yielded high cluster efficiencies regardless of the geologic target, even with a large number of clusters (15 clusters per stage). By increasing clusters per stage, the operator is now able to complete wells with fewer stages, resulting in shorter operational time and reduced cost, while maintaining or increasing production. This paper presents a comprehensive evaluation of completion diagnostic measurements and the subsequent integration of these measurements with detailed geologic characterizations and "stage level" well performance evaluation. This multidisciplinary approach resulted in more reliable completion optimization decisions and a shorter cycle time from measurement to implementation.

Introduction

While horizontal well completion designs have evolved, utilizing diverse completion methodologies across multiple basins, the main goal has remained constant: maximize individual well and/or drill space unit (DSU) value. This goal is typically achieved by optimizing the proportion of effective fractures along the lateral portion of the wellbore through the effective distribution of completion fluid and proppant within each perforation interval. Some methods utilized to achieve this goal include: near-wellbore diversion (pods or balls), far-field diversion (polylactic acid particulate), tapered gun string design, perforation angle/phasing, limited entry (LE), and eXtreme Limited Entry (XLE). The XLE designs for this work targeted a perforation friction pressure of 1500-2000 psi. For this paper, XLE was implemented in two separate DSUs in two different regions of the Williston Basin. Following completions, both batches were evaluated with multiple diagnostic techniques, including carbon fiber optic rod, downhole camera technology, step-down tests, and radioactive tracers.

The two batches of wells discussed in this paper are located in Williams County within the Williston Basin, North Dakota, which is an intra-cratonic basin that began forming during the Late Cambrian. The basin is centered over northwestern North Dakota but spans parts of South Dakota, Montana, Saskatchewan, and Manitoba (**Figure 1**). The hydrocarbon production in the Williston Basin consisted only of conventional reservoirs until the late '70s, when operators started targeting the Upper Bakken Shale with varied results. The development of the Bakken Petroleum System (BPS) began with the discovery of the Elm Coulee Field in 2000, followed by the large-scale development of the unconventional reservoirs of the BPS.

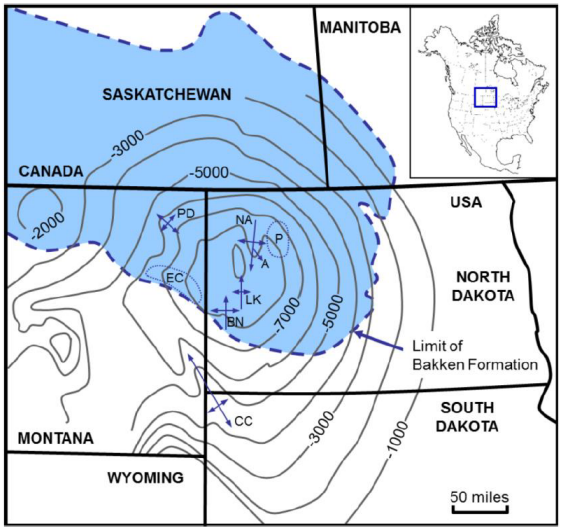

Figure 1: Map showing the extent of the Williston Basin in North Dakota and elsewhere in North America, from Pilcher et al (2011)

In this unconventional space, oil is produced from Devonian-Mississippian age tight reservoir rocks of the Bakken Petroleum System (BPS), a hybrid system with both conventional (separate source rock and reservoir) and unconventional (tight reservoirs and sources acting as seals) elements (**Wright et al., 2019**). This BPS comprises from bottom to top (**Figure 2**):

- Three Forks reservoir (TF), with alternating dolo-mudstones and dolo-siltstones; consists of several benches separated by mudstone units; in our case study, wells targeted the first bench (TF1)
- Lower Bakken Shale (LBS), acting as a source rock expelling hydrocarbons downward into the Three Forks and upward into the Middle Bakken and also acting as a top seal in most places
- Middle Bakken reservoir (MB), a mixed carbonate-siliciclastic unit with predominantly siltstones; in this case study, wells targeted the sequence boundary in the middle of this reservoir, at the interface between Middle Bakken 1 (MB1) and Middle Bakken 2 (MB2)
- Upper Bakken Shale (UBS), an organic shale source rock expelling hydrocarbons downward into the Middle Bakken and also acting as a bottom seal for the MB

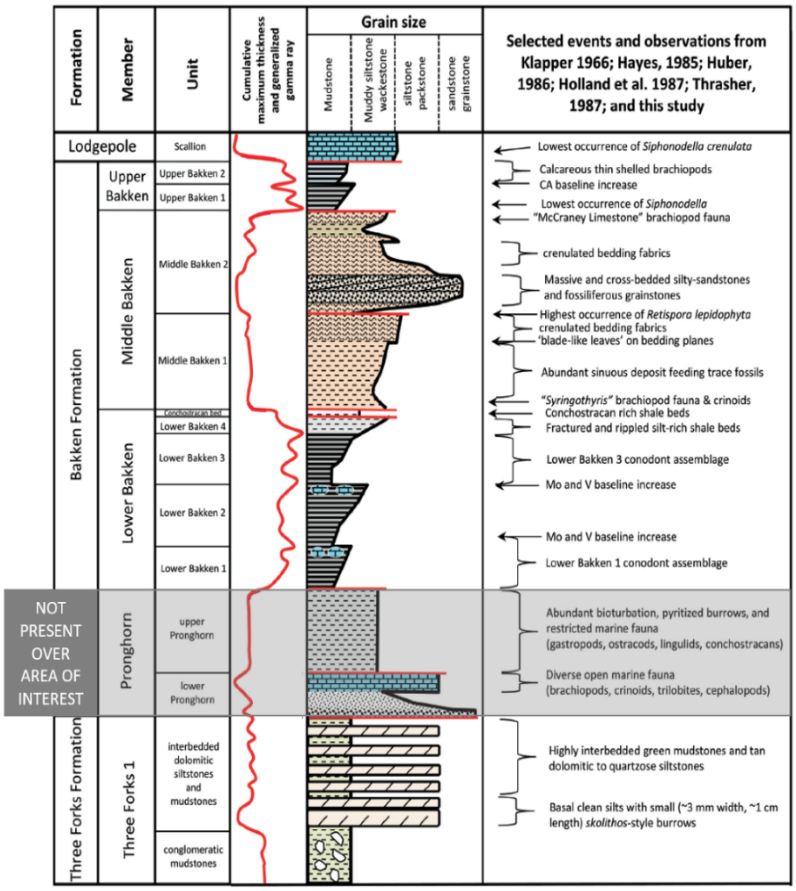

Figure 2: Generalized stratigraphic column of the Bakken Formation in the study area with selected geochemical, petrophysical, and biostratigraphic events labeled at their stratigraphic position. Red lines on the stratigraphic column indicate unconformity contacts. Modified after Hogancamp and Pocknall, 2018

Hydrocarbons from the BPS are produced from the low permeability MB and TF reservoirs via large hydraulic fracture stimulation treatments. Wells in this case study were drilled horizontally and in a wine-rack pattern in MB and TF with spacing between wells of 550 to 600ft. They were subsequently stimulated using XLE plug and perf (P&P) hydraulic fracturing. Since the reservoirs within the BPS are relatively thin in comparison to the induced hydraulic fractures, it becomes essential to optimize surface area of the hydraulic fractures within the reservoir rock, minimize sparse, overlapping, and out-of-zone hydraulic

fractures to drain each reservoir effectively. The spacing between wells and completion methods are significant variables that can be adjusted to optimize development. An additional variable that could impact production is lateral targeting. It is essential to evaluate whether well placement within the target interval has any incidence on completion and well productivity.

Limited Entry Technical Review

The underlying principles of XLE are the same as those of Limited Entry (LE) and is defined as the following:

> The process of either limiting the number of perforations or reducing the perforation entry-hole diameter in the casing to achieve significant perforation friction pressure during a hydraulic fracturing treatment. Perforation friction establishes a backpressure in the wellbore that helps to allocate flow among multiple, simultaneously-treated perforation intervals or clusters that have differing fracture propagation pressures (Cramer et al. 2019),

With LE, Lagrone and Rasmussen (1963) demonstrated with radioactive tracer and production data analysis that when the number of holes in a stage is limited, it allows for more even distribution of proppant laden fluid across an interbedded shale or sand formations. Lagrone and Rasmussen (1963) stated, "Best results are obtained by maintaining perforation friction at a maximum during the treatment". This recommendation has been supported in many publications (Cramer 1987, Eberhard and Schlosser 1995, Somanchi et al. 2016, Weddle et al. 2018). It refers to perforation erosion that takes place as proppant laden fluid passes through the perforation. Somanchi et al. 2017 and Weddle et al. 2018 provide additional details on XLE, describing how friction pressure is maximized within current operational treating pressure limits to counteract the perforation erosion that occurs during the hydraulic fracturing operations.

The equation utilized to predict the perforation friction pressure drop (**Equation 1**) is based on the Bernoilli theorem (McClain 1963, Bernoulli Theorem):

$$P_{pf} = \Delta P_p = \frac{0.2369 \times Q^2 \times \rho}{N_p^2 \times D_p^4 \times C_d^2} \qquad \textbf{Equation 1}$$

P_{pf} = Perforation Friction (psi)

ΔP_p = Pressure drop across a perforation(s) (psi)

Q = Total flow rate (bbl/min)

ρ = Density of fluid (lb/gal)

N_p = Number of open perforations

D_p = Diameter of perforations (in)

C_d = Coefficient of discharge

The design of an XLE hydraulic perforating operation must quantify and account for variability in the following parameters, identified by Weddle et al. (2018):

1. Minimum horizontal stress variability along the lateral
2. Near-wellbore friction variation from stage to stage and perforation to perforation
3. Stress shadowing between active clusters
4. Fracture extension pressure variability based on changes to net pressure
5. Perforation friction initial condition variability limiting ability to achieve designed pump rate
6. Perforation friction changes during frac stage

For an excellent guide to how each of these design factors can be quantified, please reference Weddle et al. (2018).

Weddle et al. 2018 further describe the decrease in variability of these parameters by utilizing XLE with a 1,500 psi friction pressure vs. the variability when using 500 psi friction pressure. The Injection Variability Index, **Figure 3**, reveals a reduction in variability of injection as perforation friction increases to 2,000 psi and above.

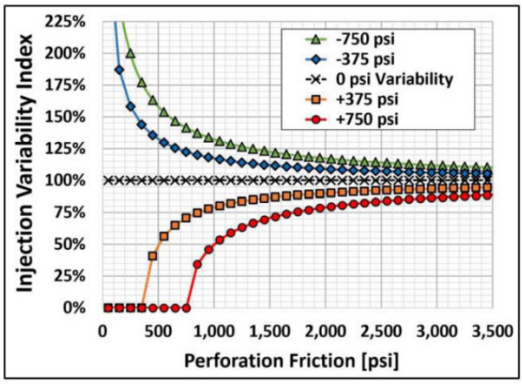

Figure 3: Injection Variability Index, the ratio of baseline injection rate, 0 psi variability in intra-stage fracture-entry pressure, to the injection rate associated with variation in fracture-entry pressure eat other entry points/clusters. (Weddle et al. 2018)

Friction of 2,000 psi should be targeted, with the assumption that a pressure drop of approximately 500 psi to account for perforation friction changes during the frac stage (Weddle et al. 2018). This perforation friction pressure target was utilized in wells evaluated in this paper.

Weddle et al. 2018 showed that Perforation cluster efficiency (PCE) from radioactive (RA) tracer data were positively impacted in XLE wells with a PCE of 80% for 15 cluster stages. Post-frac fiber optic distributed temperature sensing (DTS) and distributed acoustic sensing (DAS) were deployed in the same study, indicating an 80% average production cluster efficiency across all XLE stages (Weddle et al. 2018).

Completions and XLE design parameter

In this paper, the operator presents case studies from 2 DSUs in separate areas of the basin (SC-DSU and CA-DSU) (**Figure 4**).

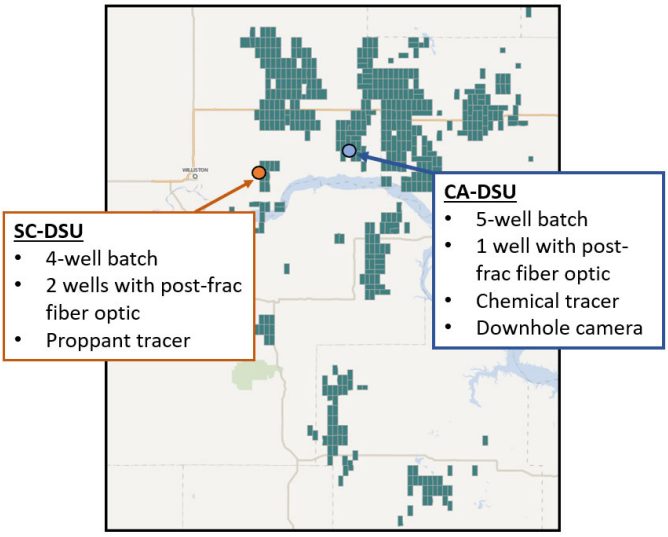

Figure 4: Drilling Space Unit (DSU) location

The SC-DSU consists of 4-wells that were completed with a plug and perf design using 18MM lbs. of proppant, 48 stages, and 360 clusters per well. To reduce completions cycle time, thereby reducing costs, the operator increased the number of clusters per stage while optimizing the number of fracturing stages. XLE design was trialed, and several diagnostic tests were carried out in the 3000-ft heel section of the laterals on two wells (SC-H2 and SC-H3). Stages with 6-8 clusters were designed with 800-1,000 psi of perforation limited entry pressure and trialed XLE stages with 10-15 clusters were designed with 1,500-2,000 psi of perforation limited entry pressure. To minimize the geological effect of each type of the limited entry design, the non-XLE stages and XLE stages were alternated in the lateral. The type of completion data gathering methods used in these wells are:

- Proppant tracers; the tracers were pumped in alternating stages in the heel-half of the well
- Post-fracture deployable fiber optic rod; the fiber optic unit was run once the wells were on natural flow period to collect Distributed Acoustic Sensing (DAS) and Distributed Temperature Sensing (DTS) data
- Step down tests conducted before and after the stimulation stages to calculate limited entry pressure and the number of opening perforation holes

The objective of the CA-DSU diagnostic plan was to confirm and validate the result from the SC-DSU before expanding XLE design as a standard design going forward in all developing batches and wells. The CA-DSU is a 5-well batch and was completed with a plug and perf design using 12.8 MM lbs of proppant, 42 stages, and 320 clusters per well in 4 out of 5 wells in the batch. The H5 well was designated as a diagnostic well with XLE design in all stages with a calculated limited entry pressure of 2,500 psi. This well was completed with 12.8MM lbs of proppant, 29 stages, and 320 clusters. In this batch, XLE completions design helped reduce 11 stages from the standard configuration. The completions design evaluation utilized chemical tracers, DAS and DTS from fiber optics, and downhole camera imaging to help characterize erosion in each perforation.

DSU	Well	Total Proppant (MMlbs/well)	Total clusters/well	Stages	Avg clusters spacing (ft)	LE pressure (psi)	Completion Design	Data Gathering well
SC-DSU	SC-H2	18	360	48	26	1500	XLE heel stages	Yes
	SC-H3	18	360	48	26	1500	XLE heel stages	Yes
	SC-H4	18	360	48	26	1500	XLE heel stages	
	SC-H5	18	360	48	26	1500	XLE heel stages	
CA-DSU	CA-H5	12.8	320	29	30	2000	XLE in all stages	Yes
	CA-H6	12.8	320	42	30	800	non-XLE	
	CA-H7	12.8	320	42	30	800	non-XLE	
	CA-H8	12.8	320	42	30	800	non-XLE	
	CA-LE-H1	12.8	320	42	30	800	non-XLE	

Table 1: Completion Design Summary

DSU Level Geology

The thickness and petrophysical properties of the reservoirs and source rocks vary across the basin. The cross-section in **Figure 5** shows both areas have a ~120ft section from the base TF1 reservoir to top UBS. In this case study, wells target either the MB reservoir or the TF reservoir. Reservoir pressures are higher in the SC-DSU with ~8,700psi of pressure versus pore pressure in CA-DSU of ~6,200psi.

Middle Bakken

The MB formation is a mixed siliciclastic-carbonate reservoir that sits, stratigraphically in-between the two source rocks (**Figure 2**). The SC-DSU exhibits a 45ft thick MB section compared to 52ft at the CA-DSU. The two areas show similar petrophysical properties with average porosities of 6-7% in MB, but with some stratigraphic variability due to variation in grain size and bedding fabrics. These differences in grain arrangements result in varying permeabilities in the different units (estimated to be 100 to 4,000nD). Water saturations are very similar in both areas (40 – 60%).

Middle Bakken wells generally target the sequence boundary between Middle Bakken 1 (MB1) and the Laminated MB2, but typically porpoise between these two units along the length of each well. Below the sequence boundary, in MB1, the rocks are very fine-grained sandstones arranged in laminae. In contrast, above the sequence boundary, in the Laminated MB2, the rock consists of fine-grained thinly laminated sandstones to siltstones, transitioning up to massive and cross-bedded silty sandstones and fossiliferous grainstones of the Massive MB2. The wells did not cross the upper part (MB2) in this case study but stayed largely in MB1, the Laminated MB2, and Massive MB2.

Three Forks

The TF reservoir consists of dolomitic siltstones and mudstones below the LBS. Unlike the MB, the TF1 is just a few feet thicker to the West in the SC-DSU (26ft vs. 29ft), but the overall thickness is very similar in both DSUs.. Vertical variations are observed in the TF1 where porosities can be as low as 1-3% at the base in the more massive Basal Clean silts (TF1 Basal Clean) and increase upward to 9% in the interbedded dolo-mudstones and dolo-siltstones (TF1 Interbedded) (**Figure 5**). Permeabilities range from 100 to 4,000nD, depending on clay content, which can lower permeabilities considerably. Water saturations are also very similar in both areas, ranging from 40% to 80%, where clay-rich dolomitic mudstones contain high water saturation. The TF benches below TF1 are saturated with water, which puts the wells targeting the TF1 in close proximity to the water leg.

Three Forks wells usually target the interface between the more massive unit at the base, TF1 Basal Clean, and the overlying TF1 Interbedded unit. But across the length of the lateral, wells also intersect the underlying water-saturated mudstone unit (TF1 Mudstone), which is more clay-rich and exhibits much lower permeabilities in the 10-1,000nD range.

Figure 5: Cross-section of two wells near the areas of interest

Shales

The UBS and LBS are also very comparable in both areas in terms of thickness (UBS is 15 to 18ft; LBS is 25 to 27ft) and petrophysical properties. Porosities range from 6-7%, and permeabilities are estimated to be 20 to 1,000nD from crushed rock analysis. These values are believed to be optimistic and dependent on the core analysis technique. Water saturation in these source rocks is 20-30%.

As wells intersect different rock types within each formation, it becomes crucial to evaluate the impact of initiating hydraulic fractures in these various units and understand the implications for hydraulic fracture effectiveness. This case study aims at determining whether the various petrophysical and geomechanical properties in the different units affect the effectiveness of the completion job and the productivity of the rock (**Table 2**).

		SC-DSU					CA-DSU				
Zone	Lithologic Description	Thickness (ft)	Porosity (%)	Water Saturation (%)	YM (MMpsi)	PR	Thickness (ft)	Porosity (%)	Water Saturation (%)	YM (MMpsi)	PR
MIDDLE BAKKEN											
WAVY BEDDED MB2	Very fine sand with minor to moderate carbonate grains	8	5.4	68	6.9	0.15	NOT DISCUSSED IN THIS PAPER				
MASSIVE MB2	Mixed very fine to fine grained sandstone and ooid/peloid grainstone	6	7.6	47	8.8	0.18					
LAMINATED MB2	Mixed very fine to fine grained sandstone and ooid/peloid grainstone	2	6.4	56	7.6	0.17					
LAMINATED MB1	Very fine to fine grained sandstone, minor to moderate carbonate grains	11	5.8	63	7.5	0.16					
BIOTURBATED MB1	Very fine to fine grained sandstone with scattered thin-shelled brachiopods	19	6.0	65	7.5	0.16					
THREE FORKS											
TF1 INTERBEDDED	Silty to sandy (very fine) dolomite interbedded with argillaceous dolomitic mudstone	19	7.5	62	7.9	0.15	20.0	6.8	59	7.4	0.16
TF1 BASAL CLEAN	Silty to sandy (very fine) dolomite with less gray-green silty shale drapes	7	4.3	36	7.9	0.17	9.0	5.1	52	7.6	0.16
TF1 MUDSTONE	Red-brown dolomitic, silty mudstone	15	6.4	100	6.8	0.16	11.0	4.7	98	6.9	0.16

Table 2: Summary table of petrophysical and geomechanical properties in the areas of interest

Completions Diagnostic Technology

Multiple types of diagnostic tools and techniques were used to evaluate completion efficiency in the diagnostic wells. The timing of diagnostic deployment ranges from concurrent with the fracturing operation to after well cleanout operation, and stable flow is achieved.

Proppant Tracers

The proppant tracers or Radioactive tracers (RA tracers) employed are ceramic beads, which utilize low-level gamma-emitting tracers (Iridium-192, Scandium-46 and Antimony-124). The tracer is an integral part of the ceramic bead and does not wash away. The tracers are injected throughout the proppant-laden section of a stimulation treatment. Post-completion, a spectral gamma-ray log, is run to identify and quantify individual tracer types in the near-wellbore region. An estimated depth of investigation of this tool is 2-ft around the wellbore. The tracers are identified in the logs by their red (Ir-192), yellow (Sc-46), and blue (Sb-124) signatures (Woodroof et al. 2003). Typical uses of proppant tracers include evaluating proppant coverage across a lateral, unstimulated perforation clusters, near-wellbore fracture complexity, cluster and stage spacing, diversion effectiveness, zonal containment, fracture height and fracture type (transverse/ longitudinal) (Senters et al. 2015).

The proppant tracers were pumped in all three diagnostic wells (SC and CA project) and in alternating stages during the fracturing operation. This alternating between stages technique results in clear visible stages without proppant tracer in between stages with tracers, which allows the operator to evaluate better contamination between stages, plug leakage, and performance of each cluster. **Figure 66** shows the lateral coverage of each type of diagnostic tool.

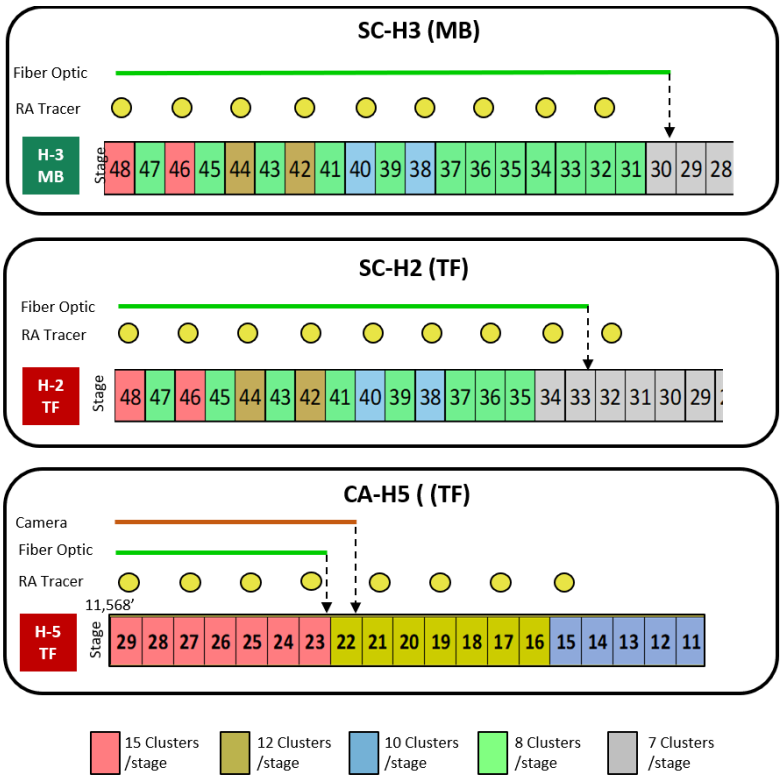

Figure 6: Completion Diagnostics Deployed on Each Well and Lateral Coverage

Post-Fracture Deployable Fiber Optic

Post-fracture deployable fiber optic technology enables temporary deployment of fiber optics into unconventional wells. A spool of carbon fiber rod, with optical fibers inside, is deployed and/or tractored into a well for acoustic (DAS), and temperature sensing (DTS). Additional detailed information on deployable fiber optic sensing can be found in Ahmed Attia et al. SPE-194338.

The acoustic information is used to understand and characterize the flow regime and production types, to look for crossflow or well integrity issues, and to qualitatively determine production allocation. This detailed information about well and reservoir behavior provides an essential constraint in a two-phase temperature model, which would otherwise give a non-unique solution, allowing production quantification at the cluster level.

Post-fracture deployable fiber optics data were gathered while the three diagnostic wells were flowing naturally. The measurements were used to evaluate completions efficiency from the XLE and normal LE pressure stages. Since a tractor was not used in this project, due to physical wellbore limitations, the investigation was limited to between 4,500 to 5,500 ft into the lateral section. In the SC-DSU the fiber optic rod covers between 15-18 stages, and in the CA-DSU the fiber optic rod overs only seven stages. This was due to the CA-DSU utilizing XLE design though out the whole lateral, which allows larger stages that cover more lateral length of the well.

Downhole Camera Technology

Downhole camera technology has been widely used in the industry for what could be classed as reactive downhole events such as wellbore restriction, and casing deformation evaluation. Recent work by Cramer et al. (2019) indicates the extensive technical benefit of using video-based data acquisition for the purpose

of perforation imaging and video analytics to evaluate the effectiveness of the limited entry perforation program. The array side-view camera for 360° logging is used for perforation imaging; this tool can be deployed by various means including wireline, E-coil (real-time), or regular coiled tubing (memory mode). The side-view footage is captured continuously in a 360-degree view around the tool at 25 frames/second and a video resolution of 2880 pixels x infinity (>5 gigapixels processed per 30ft).

The downhole camera was only deployed in the CA-H5 to visualize perforation and validate the data from the fiber optic and proppant tracer diagnostics. The camera was deployed after fracturing and coiled tubing cleanout/mill out (CTCO) operation was completed. The tool used in this well was a memory style tool with 6 hours of continuous recording capacity. After all data was collected, and the tool was retrieved and the data was then downloaded and processed.

Step Down Test Results

Step-Down tests were utilized in conjunction with the other data gathering techniques for XLE evaluation. Step down tests were performed at the beginning and end of the frac stage and provided more detail to the analysis and aid in characterizing the effects of erosion and/or other treatment issues (Wright 1997). The goal of the step-down test is to 1) Determine if LE pressure targets are being met 2) Determine if those LE pressure targets are maintained throughout the stage and 3) Gauge the achieved cluster efficiency by estimating the number of open perforations. See

Figure **7**, for example, plots of the data points and the regression results.

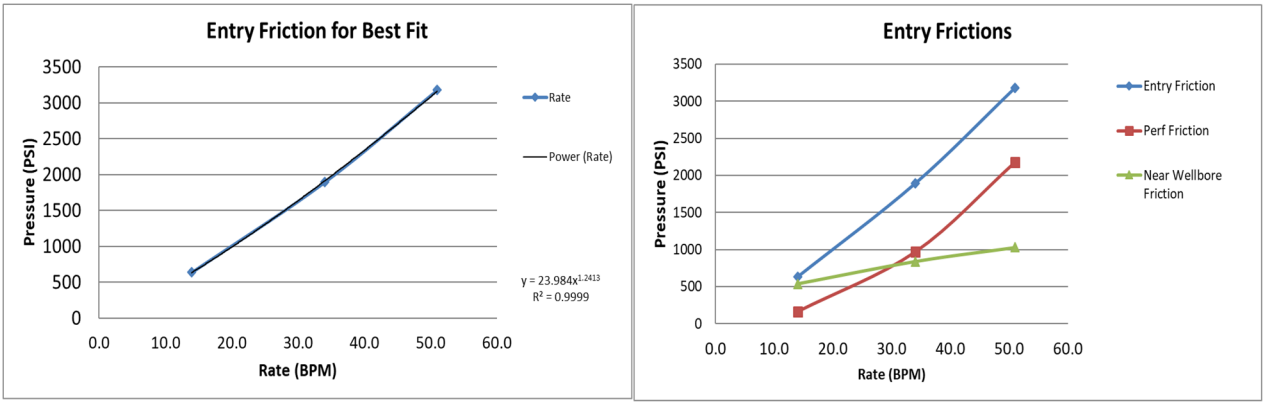

Figure 7: Step Down Test Data Points & Regression Analysis, Pressure (Psi), Rate (Barrel/min)

The analysis presented within this paper utilized flow loop testing of Friction reducer (FR) at 1 **gallon per thousand (**gpt) and 4gpt to estimate friction pressures. Requirements of the test are 3-5 data points at a steady rate, pressure and an ISIP (Instantaneous Shut-In Pressure). See **Figure 8** for an example of an implemented test.

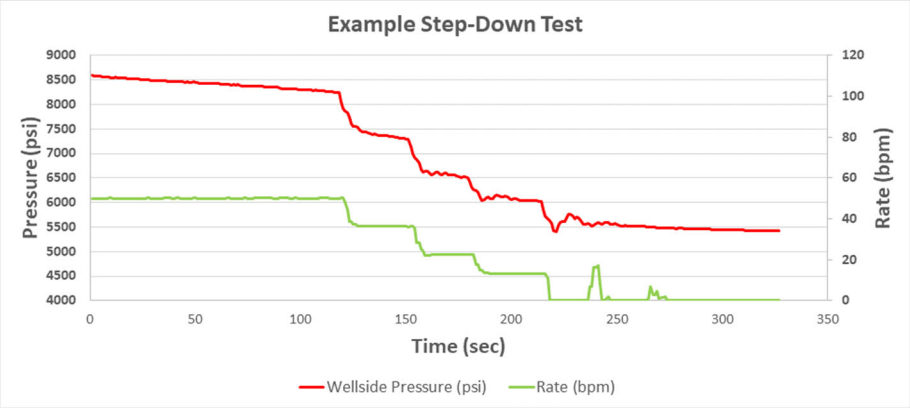

Figure 8 Step-Down Test Example

The perforation design of the SC-H2 well targeted limited entry pressures of 1,600 psi for cluster counts of 10 or more. In **Figure 9,** the pre-frac perforation friction is shown. Limited entry targets were met on 5 of the 6 test stages. In the post-frac step-down analysis, 5 of 5 stages still met the 1,600 psi limited entry target. Both goals 1 and 2 were achieved as determined by the step-down tests performed.

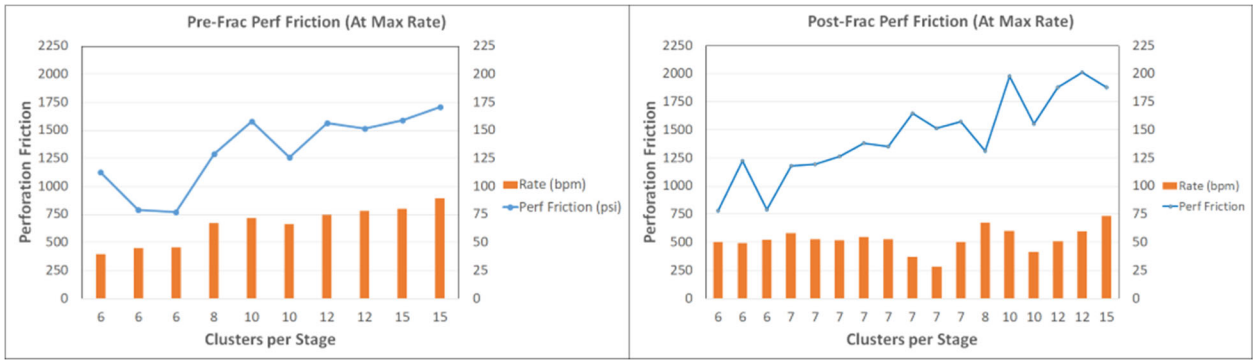

Figure 9: SC-H2 Pre & Post Frac Perforation Friction (psi)

Further testing of 15 cluster stages was implemented on the CA-H5 completion and are displayed in Figure 10. A similar step-down analysis was completed in order to evaluate the XLE performance. A different perforation charge was utilized on the CA-H5 than the SC-H2 resulting in a smaller entry hole diameter (EHD) and an increased perforation friction pressure. The range of calculated friction pressure was from 1,600 psi to 3,300 psi, averaging 2,700 psi. The higher friction pressure reduced the achievable rates relative to the SC-H2. No pre-frac step rate tests were performed, but given the trend from the SC-H2 data, it is likely that the limited entry targets were maintained throughout the stage.

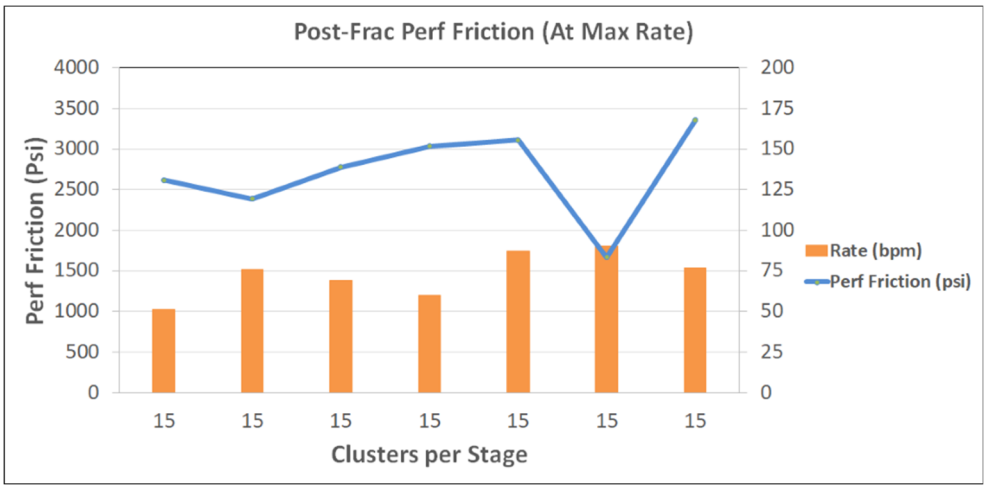

Figure 10: CA-H5 Step-Down Test Results

It should be noted that the SC-H2 post-frac step-downs showed that the limited entry targets were met at a lower rate than the pre-frac tests. Reduced pump rates as well as perforation erosion should both result in a decreased limited entry pressure, therefore the most likely change that also occurred throughout the frac is a reduction in the number of perforations. **Figure 11** illustrates the change in the estimated number of open perforations between the pre-frac and post-frac step down tests.

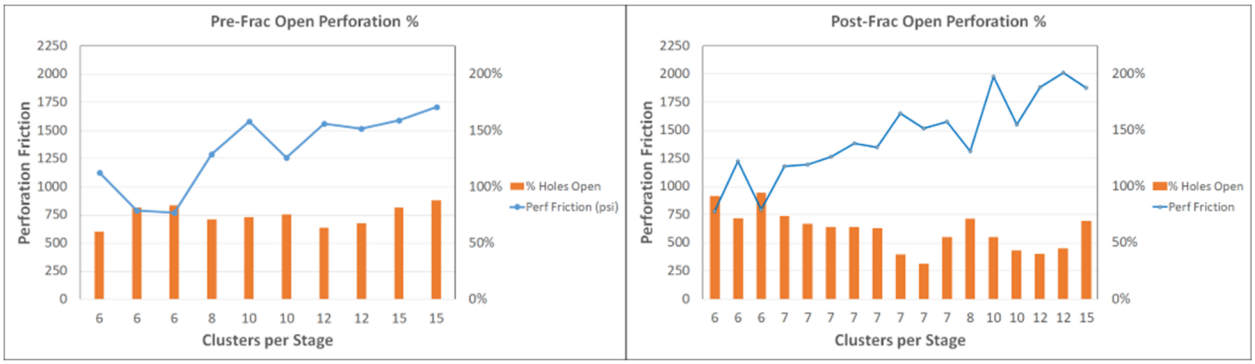

Figure 11: SC-H2 Estimated Open Perforations

The reduction in open perforations throughout the frac treatment could be problematic and lead to uneven fluid distribution throughout the clusters. The third goal mentioned in this section is to gauge the relative cluster efficiency of the fracture treatment. Given the data presented, the cluster efficiency could range from 50% to 100%. The number of open perforations still leaves the potential that all clusters were taking fluid throughout the treatment, and further data gathering, including RA tracer and fiber optic sensing, can provide another level of detail for cluster efficiency evaluation not available with a step-down test.

Proppant Tracer Results

Proppant tracer results were collected during coiled tubing cleanout operation with a spectral gamma-ray logging tool. The operator uses data to determine completions efficiency which is defined as proppant placed in each cluster versus the total clusters planned in a stage. In the SC-H2 well, the operator traced this well with Scandium-46 (yellow), and the coiled tubing spectral gamma-ray logged from stage 32-48 stages (9 stages with tracers). The tracer log results are shown in Error! Reference source not found.**14**. Stages with 7-8 clusters show 100 % cluster efficiency, (tracers show in all of the clusters). The stages with

10 clusters show 80% efficiency (clusters show in 8 of the 10 clusters). Stages with 12 clusters show 92% cluster efficiency (11 out of 12 clusters), and stages with 15 clusters show 100%. In the SC-H2 stage with 15 clusters, it is evident that there is a plug leak, indicated in Figure 12**,** with a red triangle.

For SC-H3, the well was traced with two types of tracer, Iridium-192 (red) and Antimony-124 (blue). Two tracers were used sequentially to understand the early versus late proppant placement. Nine stages were logged with spectral gamma-ray in this well. Stages with 8-12 clusters show 100% cluster efficiency. However, stages with 15 clusters show 93% clusters efficiency. Figure 12 shows the proppant data log for SC-H3. SC-DSU data indicates that the XLE stages (10-15 clusters) show similar results to that of the stage non-XLE design.

For the CA-H5, the well was traced with all three types of tracer: Scandium-46 (yellow), Iridium-192 (red), and Antimony-124 (blue). Eight stages were logged with spectral gamma-ray in this well. All stages in this well were completed using XLE design. The average cluster efficiency in the 10 cluster stages is 90%. In stages with 12 and 15 clusters, the efficiency is down to 72% and 77%, respectively. In both cases, this is likely due to the plug leak issues, which are also captured by the RA tracer. If the plug leakage data was removed from the data set, the average cluster efficiency is an acceptable range of approximately 90%.

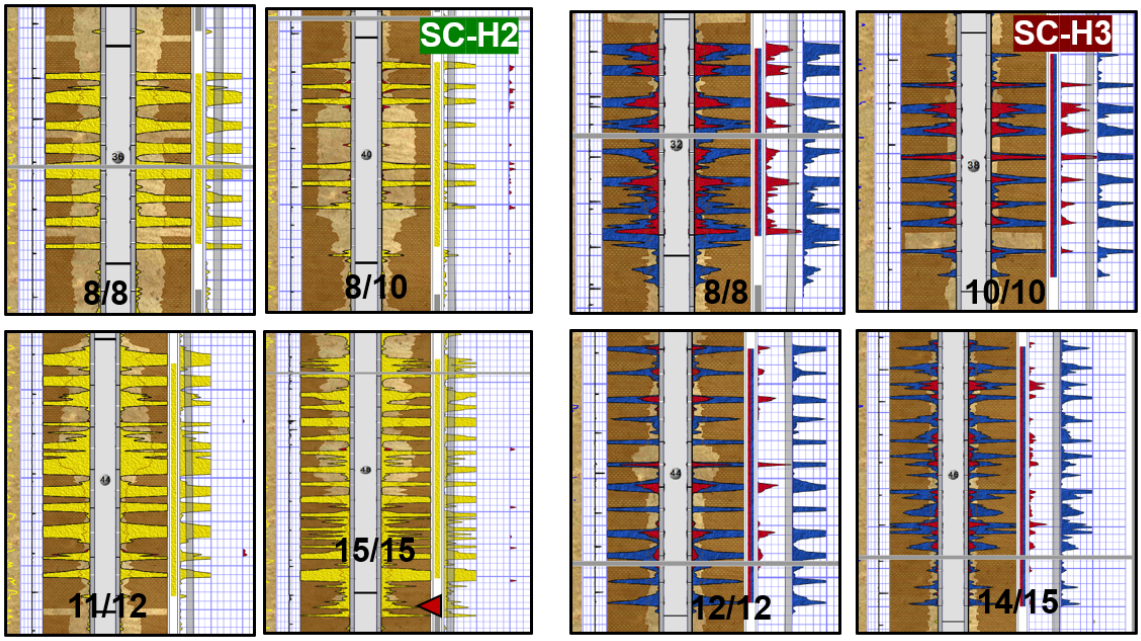

Figure 12: SC-H2 Proppant Tracer Logs, Scandium-46 (yellow) and SC-H3 Proppant Tracer Logs, Iridium-192 (red) and Antimony-124 (blue)

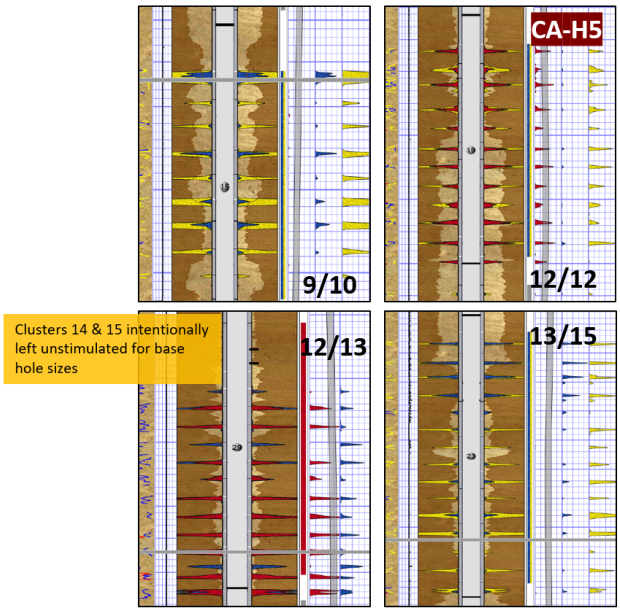

Figure 13: CA-H5 RA Tracer Log. Scandium-46 (yellow) and SC-H3 Proppant Tracer Logs, Iridium-192 (red) and Antimony-124 (blue)

Post-Fracture Deployable Fiber Optic Results

Post-fracture deployable fiber optic data was acquired ~6 months after the well was first brought online on the SC-DSU and ~4 months after for the CA-DSU. These times were selected to ensure that the well was in a stable flowing condition during the data collection operation. The post-fracture deployable fiber optic operation objective is to acquire DAS & DTS data and then translate it to completions efficiency results for LE and XLE analysis. This operation takes approximately 60 hours per well. The data acquisition sequences include run in hole while producing, alternating between shut-in and production periods (**Figure 14**), 24-hour shut-in period, POOH, and rig down. The acoustic and temperature data were then analyzed to help estimate production and completions efficiency.

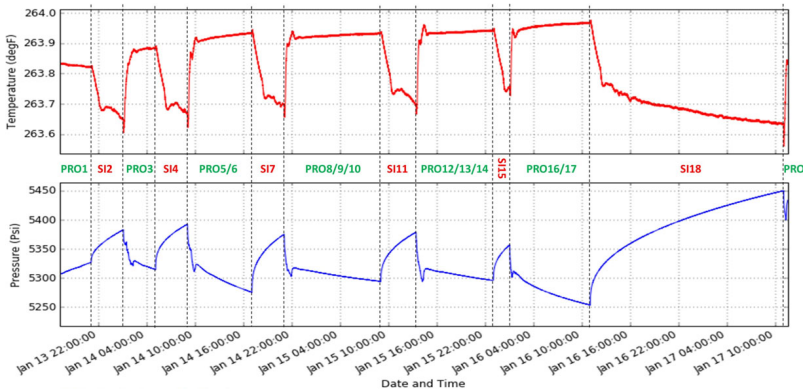

Figure 14: DAS & DTS Data Capturing Sequence (PRO = Producing; SI = Shut-in)

The deployable fiber optic rod was able to capture 16 stages in the SC-H2 (approximately ½ of a lateral without the use of a tractor). The data was then analyzed and interpreted using an inverse temperature model with the acoustic data used to constrain the model to provide production data on a cluster level. **Figure 15** shows a summary data from the deployable fiber optic rod (DAS & DTS data) for the SC-H2. The summary

plot shows temperature data, shut-in (SI) pressure data, shut-in temperature data, flowing pressure, frequency of the acoustic from each lateral, frequency range, true vertical depth (TVD), production noise ranking, and production distribution of water and oil calculated with PLATO temperature modeling software.

Figure 15 track 1 (from bottom-up), the solid blue line shows the temperature of the observed lateral while the well is in stable producing condition. On the same track, the solid red line indicates temperature data while the well was shut-in for 24 hours. Combined with the stable flowing temperature profile, these two traces reveal the thermodynamic relationship between cumulative production as it travels up-hole and the individual production at each cluster as they exchange heat with the surrounding environment. The shut-in temperature trace also reveals characteristics of the stimulation impact on the reservoir, reflecting variations in volumetric uniformity, proximity of stimulation fluid storage to the wellbore, fracture complexity, thermal diffusivity, and true vertical depth. Cooler temperature indicates more frac fluid injection into the lateral section, and warmer means less injection. In this case, warmer temperature data is found between stages where frac plugs are set, which shows that most of the frac fluid was injected into each stage and indicates that heel bias increases as stage length increases.

Track 2 is a snapshot of the acoustic spectrum after a transition from shut-in to flowing, where hotter colors indicate more production and vice versa. Track 3 from the bottom (greyscale) shows a 6-minute window of differential acoustic intensity (i.e., the change in noise power) as production flows in from each cluster and moves up-hole. Using this data as an input, proprietary software analyzes the intensity, duration, velocity, and direction of flow from each cluster. It assigns a rank from 0 to 5 and the production phase type (track 4). Ranking of 1 represents the lowest production, and 5 represents the highest. The colors reflect the assigned oil/water ratio, with blue clusters appearing to produce a higher proportion of heavy to light liquid (water). These ranks are then used as a constraint in PLATO temperature modeling software to quantify production (track 5 and 6).

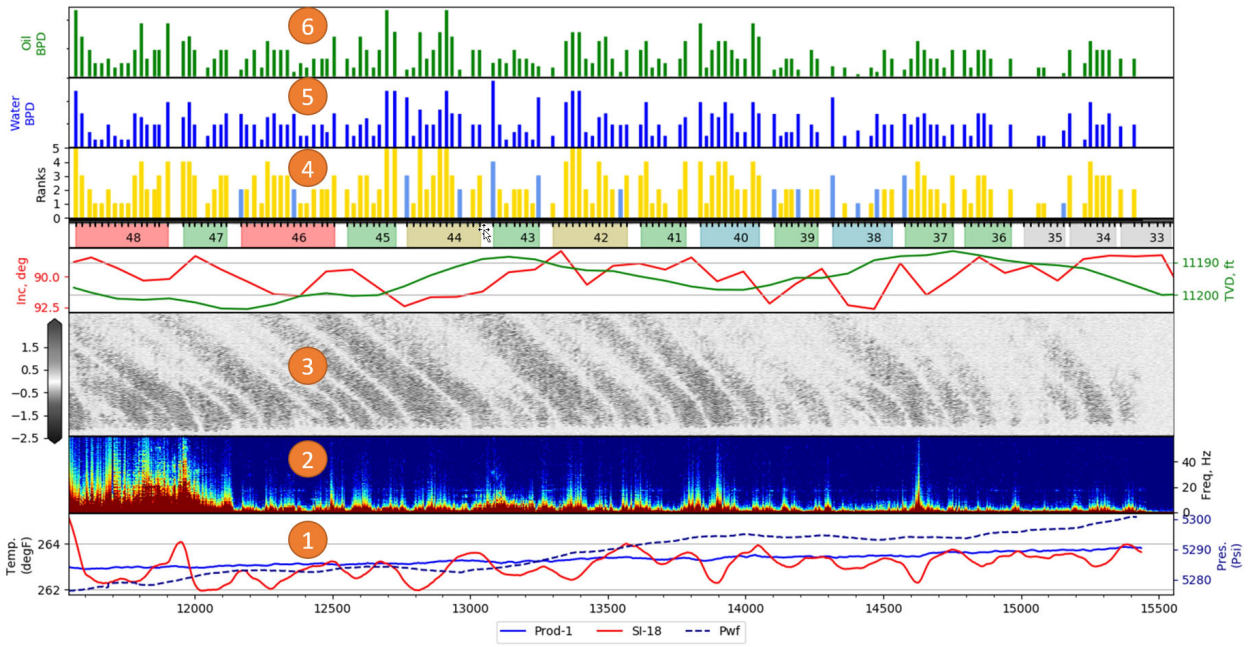

Figure 15: Summary Result from Deployable Fiber Optic Rod

Figure 16 shows a detailed fiber optic summary plot of SC-H2 stages 47 and 48. Stage 48 (XLE stage), DTS data indicates a relatively uniform shut-in temperature profile, suggesting uniform treatment of the stage. Production ranking results indicate 100% of the clusters produced, while stage 47 (non XLE) shows

88%. Overall well SC-H2 XLE stages average production efficiency is 93% while the non-XLE stages average is 85%. In this analysis, the production ranking of one or more considers them productive clusters. The non-XLE design uses 800-1000 psi limited entry design while the XLE design is between 1,500-2,000 psi.

The SC-H3 well, the fiber optic rod, was able to capture 19 stages with both XLE and non-XLE stages. The well shows similar results as the SC-H2 that the average XLE stage production cluster efficiency is 97%, and the non-XLE production clusters efficiency is 72%.

The CA-H5 XLE well, the fiber optic rod, was able to capture seven stages with a similar amount of lateral observed as the previous two wells. The XLE design allows the engineers to plan for more effective clusters in a stage that results in larger stages within a similar amount of lateral covered. The production cluster efficiency averages 92%. XLE completion design results from post-fracture deployable fiber optic consistently indicate an increase in production cluster efficiency on average from 75% to 90% over the non-XLE design stages.

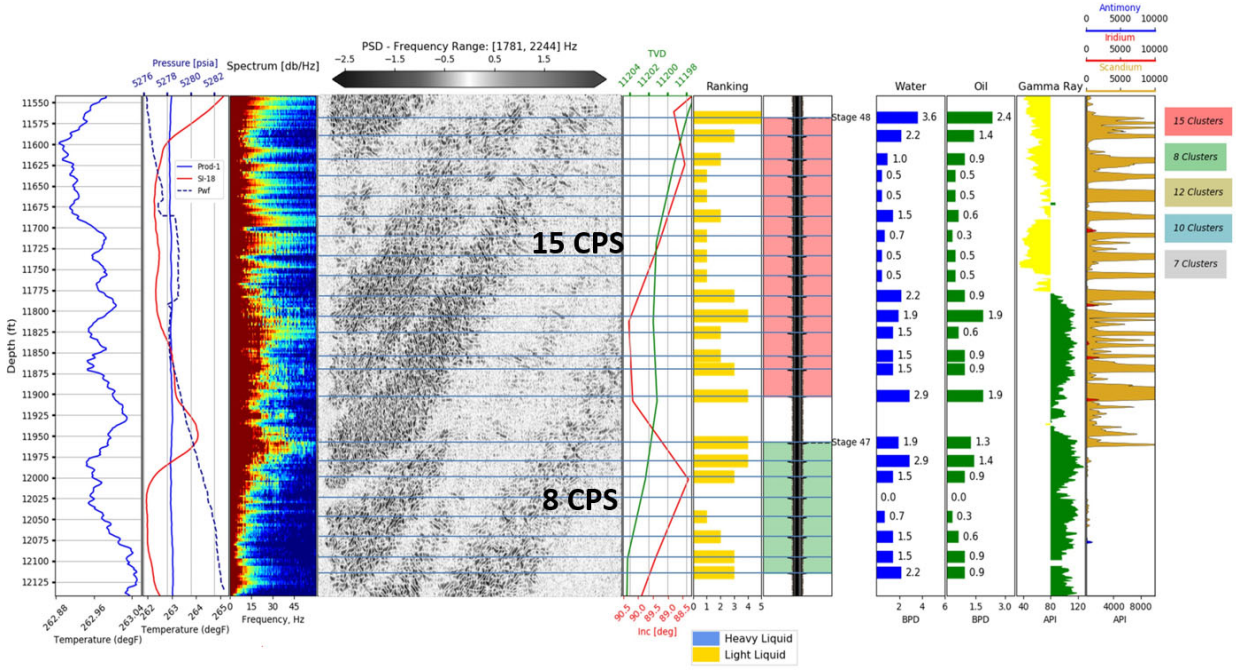

Figure 16: Detailed Summary Data of SC-H2 Stage 47 and 48

Downhole Camera Result

Following on the positive results from the SC-DSU trial and, to further capture the understanding of XLE on a perforation level, a downhole camera was run in the CA-H5 well to help identify a correlation between each type of data. The downhole camera was ran post-frac via coiled tubing. Coiled tubing operations are commonly used to mill out plugs and cleanout wells from residual sand in the wellbore after fracturing operations. After the mill out or clean out process is completed, the well is circulated with clean fluid until the lateral fluid is clear. The memory camera tool was then run in the well accompanied by a spectral gamma-ray logging tool to capture dimensions of perforations and erosion effects on perforation clusters. In the last stage of CA-H5, 2 clusters (4 perforations) were left unstimulated to create a baseline of the entry hole size. Stages with the 15 cluster perforation plan are two shots per foot (SPF) with 0.31" entry hole (EH) size at 0-180 degrees phasing. The 0.314" EH was based on 4.5" P110EC casing ran in the well. Stages with less than 15 clusters, the perforation charges used were 3 SPF, 0.31" EH, and 120 degrees phasing.

The coiled tubing with the camera and spectral gamma-ray log was able to capture eight stages, 110 clusters, and 228 perforations. **Figure 17** shows an example of perforation images captured from the downhole camera.

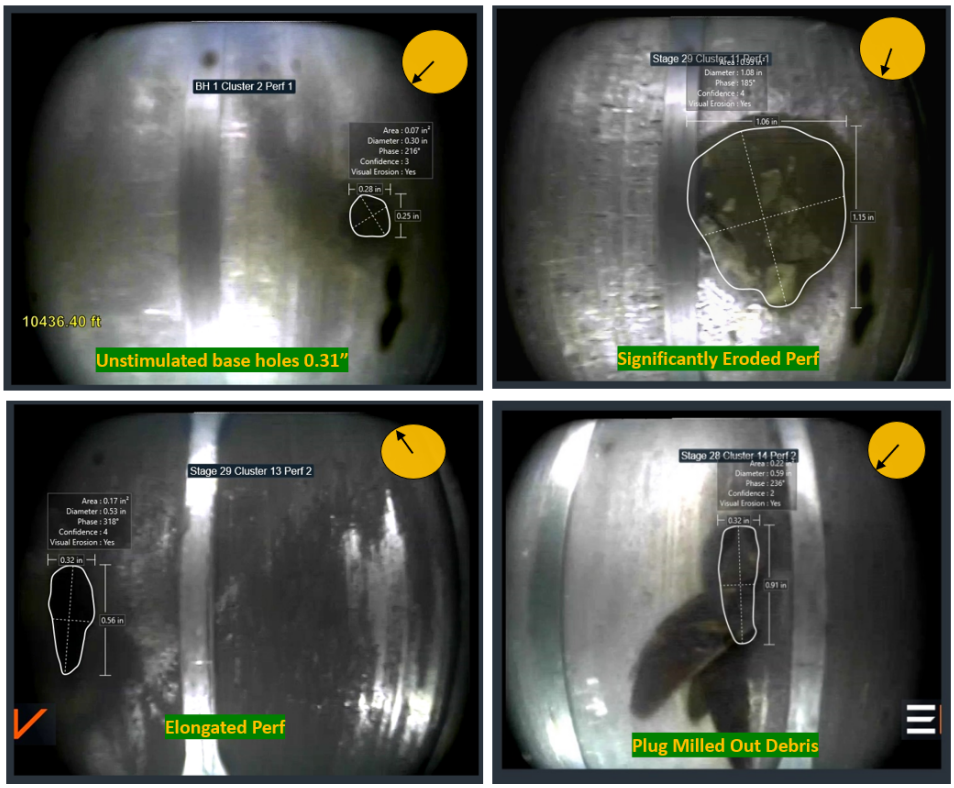

Figure 17: Images from downhole camera showing base hole, eroded perforation, elongated perforation, and plug parts left after cleanout operation

Perforation images are evaluated for erosional area and equivalent perforation diameter (Cramer et al. 2019) using image pixel calculation. The operator uses the location of each perforation to evaluate perforation bias within the stage and how each perforation eroded based on sand perforation phasing. **Figure 18** shows an example of the average perforation area bar chart from stages 27, 28, and 29. All three stages show a clear heel to toe bias of the erosional area.

On stage 28, a 2 SPF gun was planned for this stage with 15 clusters. However, the downhole imaging camera was able to capture one additional shot versus what was planned in clusters 5 and 9. The camera images indicate that these 2 clusters show a higher erosion effect when compared with other perforations in the stage. These extra perforation holes in the clusters cause uneven bias in the erosion of each cluster. This effect proves that clusters with less limited entry pressure take more fluid and create uneven stimulation stages and also elevates the importance of quality control from perforation gun manufacturing companies. The unplanned perforation shots can greatly affect fluid distribution in fracture stimulation stages.

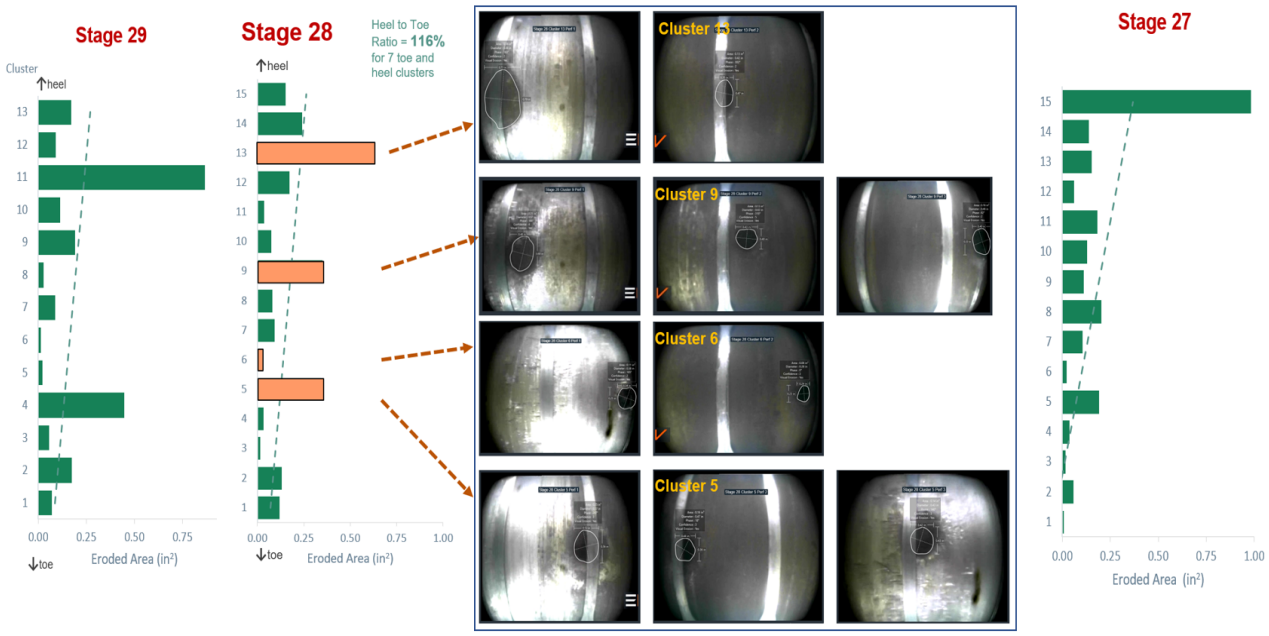

Figure 18: Bar charts show heel-toe bias in eroded area. Stage 28 highlights impact of extra shots in clusters 5 and 9.

Analysis of 108 cluster images, area, and equivalent perforation diameter indicates that 98% of the clusters show signs of erosion, and 70% of the stages show some degree of heel-toe bias. The data also suggests that 7 clusters toward the heel side have a 161% more eroded area than the rest of the clusters toward the toe. **Figure 19** shows how perforation orientation affects perforation erosion. The majority of the sizeable eroded perforation holes are found in the perforation holes that shot toward 180-degree orientation (low side of the well). This effect indicates that gravity significantly influences the perforation erosion.

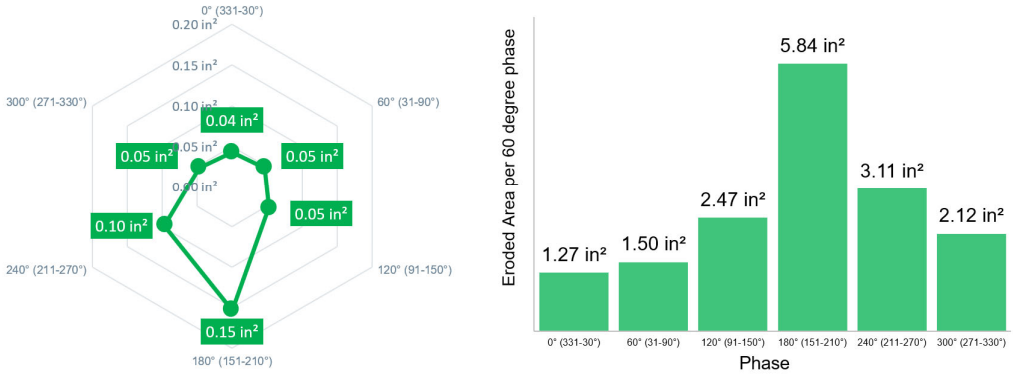

Figure 19: Erosion area vs perforation orientation

Diagnostic Results Combination

To validate cluster efficiency using multiple diagnostic methods, and to try to understand if there is a correlation between the various types of data acquired from theses trial wells, a combination of the data from post-fracture deployable fiber optic, RA tracer, and downhole camera data on the CA-H5 well was performed. The combination of the three types of the data are able to perform in 4 stages of the CA-H5 well

as the RA tracer was pumped in alternating stages, and seven stages were of data were captured from this well. Data from this well, stages 26 and 27, are shown in **Figure 20**.

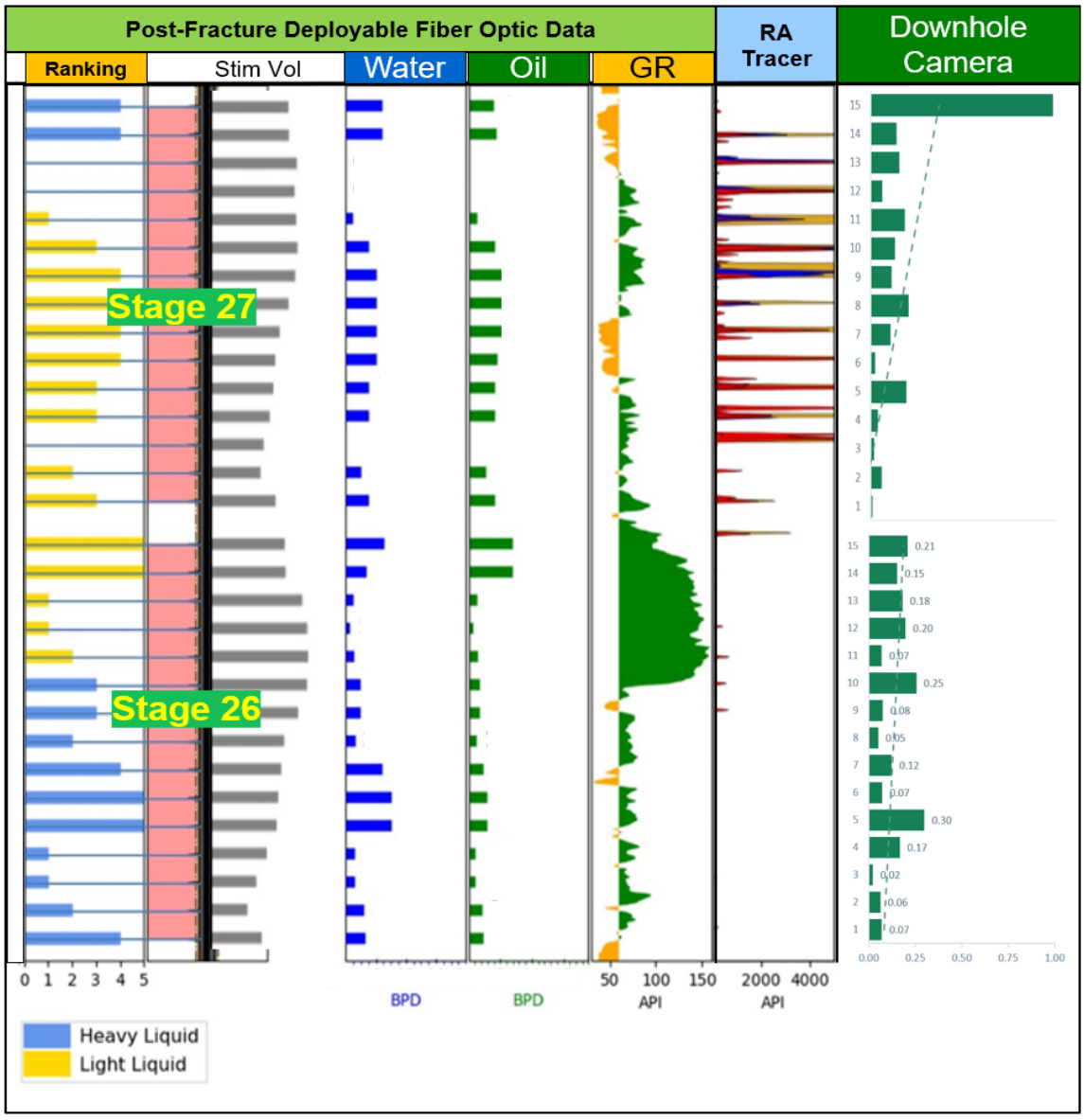

Figure 20: CA-H5 Stage 27 and 26 comparison between deployable fiber optic, RA tracer, and downhole camera erosion data.

For stage 27, the deployable fiber optic data shows productive clusters in the majority of the stages, but no production was observed from cluster 3, 12, and 13. However, these three clusters were stimulated based on RA tracer and downhole camera perforation erosion data. The downhole camera data also indicates considerable erosion by stimulation fluid in cluster 15. However, RA tracer shows no tracer residual logged from that cluster, and the fiber optic data does not show the highest stimulation volume in that cluster. The operator was able to capture four stages, with all three types of diagnostic data. However, there is no direct correlation from one data type to one another. The downhole camera indicates erosion effect on the perforation holes, but that does not necessarily translate to production data from deployable fiber optic and RA tracer data.

The discrepancy in the results is likely due to the uniqueness of measurement from each diagnostic method. The tracer log data shows if the proppant exits through the expected perforations/clusters but does not quantify the amount of proppant or injection volume. On the other hand, the deployable fiber optic data measures the dynamic changes in temperature and acoustic response pressure to estimate the relative volume of stimulation fluid injected and production from each cluster. The significant benefit here is it shows a quantifiable result which provides a snapshot of production and injection in each cluster. The downhole camera offers insight on how much proppant was pumped through each cluster by measuring erosion based on post-frac perforation hole sizes. It is clear that each type of diagnostic technique measures the different signal from the stimulated wellbore and indirectly interpret as completions cluster efficiency. There are other factors that affect these diagnostic results, such as cement uniformity, complex fracture behind pipe, crossflow between stages, and geological characteristic in each stage.

Table 3: Summary cluster efficiency data from tracer and deployable fiber optic

Well	Perforation Clusters per Stage (CPS)	Design Limited Entry Pressure	RA tracer cluster efficiency	Deployable Fiber Cluster efficiency	Stepdown Test		Downhole Camera Eroded Clusters
					% Hole Opens	Perforation Limited Entry pressure (psi)	
SC-H2	8	1000	100%	85%	54%	1,465	NA
	10	1600	80%	85%	49%	1,765	NA
	12	1600	92%	92%	42%	1,947	NA
	15	1600	100%	100%	69%	1,880	NA
	Average of XLE stages		92%	93%	53%	1846	NA
SC-H3	7 & 8	1000	100%	70%	65%	1,049	NA
	10	1600	100%	95%	78%	1,558	NA
	12	1600	100%	100%	NA	NA	NA
	15	1600	87%	97%	NA	NA	NA
	Average of XLE stages		95%	97%	78%	1,558	NA
CA-H5	10	2500	90%	N/A	NA	NA	NA
	12	2500	*72%	N/A	NA	NA	NA
	13	2500	92%	100%	NA	NA	100%
	15	2500	73%	91%	71%	2,700	94%
	Average of XLE stages		*77%	92%	71%	2,700	97%
			* Plug leak stages				

To summarize**, Table 3** shows a summary of cluster efficiency obtained from deployable fiber optic, RA tracer data, Stepdown test, and downhole camera. The RA tracer data indicates that XLE cluster efficiency is between 92%-95% (not including stages with plug leak). The deployable fiber optic shows between 92 to 97%, and the downhole camera data (only at CA-H5) shows 97% of XLE clusters efficiency. It is evident that the overall cluster efficiency results interpreted from the downhole camera, deployable fiber optic, and RA tracer for XLE stages show some level of agreement, between 92-100%. On the other hand, the stepdown test results in this project show a wider range of % hole opens from 50% to 80%. The percentage of hole open leaves the potential that all clusters were taking fluid throughout the treatment, and some perforation holes could be shut off during some point of the treatment. RA tracer, downhole camera, and fiber optic sensing data can provide another level of detail for cluster efficiency evaluation not available with a step-down test. Therefore, it is clear that the diagnostic data captured from this project indicate that XLE design provides high cluster efficiency, more than 90% in the XLE stages.

Dependency of Cluster Efficiency on Geology

The knobs that are most often turned to improve completion efficiency and increase clusters/stage improve completion are perforation hole size, pump rate, and the number of perforation holes to achieve higher perforation limited entry pressures, via XLE. In addition to XLE, perforation orientation and novel

perforating techniques, breakdown, and diversion technologies are also utilized to improve completion efficiency.

While many engineering inputs are considered when optimizing a completion, companies rarely acquire the necessary data to understand subsurface geological heterogeneity (e.g., variability in geomechanical and reservoir quality properties). Historically, most companies implement a geometric completion design where stages and clusters are equally spaced along the lateral section of the well. While this type of design seems favorable in terms of completion operation and capital efficiency, it may not be the most effective method, especially in laterally heterogeneous rock, or in wells where the wellbore straddles geologic boundaries between layers with significantly different geomechanical properties (Far et al., 2015; Ashton et al., 2013; Ganguly and Cipolla, 2012). Geologic heterogeneity along the wellbore causes lateral variability in rock properties. It thus can have a direct effect on the geometry of hydraulic fractures initiated by each cluster along the wellbore, especially in wells where the number of clusters per stage is low.

To date, research that considers geologic heterogeneity in determining the optimal completion design illustrates that geology matters and that a more variable stage spacing approach results in improved cluster efficiency and well production for wells with lower total cluster counts. The subject of these studies has been true unconventional oil or gas shale plays. While the Bakken is considered an unconventional play, it has several key differences that set it apart from the true shale plays (the reservoirs have higher permeability and are mostly absent of organic material compared to oil and gas shales). Currently, there is a lack of studies that show using a variable, or targeted stage spacing provides efficiency or production uplift in high cluster count Bakken wells. With the recent implementation of XLE and closely spaced clusters (e.g., 25 ft to 35 ft cluster spacing), geometric perforating strategies may be the best approach to address geologic heterogeneity and achieve high cluster efficiency in the Bakken.

The interdisciplinary nature of the data collected for the two DSU's presented in this paper allows the opportunity to directly measure the effects that geologic heterogeneity has on cluster efficiency in Bakken and Three Forks wells. All three wellbores presented in this paper (SC- H3 (MB), SC-H2 (TF), and CA-H5 (TF)) straddle lithologic boundaries with a variable reservoir (porosity, permeability, water saturation) and geomechanical properties (**Figure 21, Figure 5, Table 2**).

The geologic zones intersected by the lateral sections of wells SC-H3 (MB), SC-H2 (TF) and CA-H5 (TF) is shown in **Figure 21a, b, and c, respectively**. Designations of stage number, number of clusters per stage, and corresponding cluster efficiency for the SC-H3 are also posted. For each cluster that was sensed via fiber optics, both the geologic zone and a designation of whether that cluster was effective / producing (rank = 1 or greater) was captured. This data presented graphically in the form of a bar chart can be found in **Figure 22a, b, and c**. In **Figure 22,** each bar represents the total number of clusters for each well that was located within each geologic zone; the bars are colored by whether the cluster was effective (green) or ineffective (grey). The % of each effective zone vs. ineffective is displayed on the y-axis.

In well SC-H3 (MB), a heel-to-toe bias in cluster efficiency is observed with heel clusters having an average cluster efficiency of 93% and toe-ward clusters having average cluster efficiency of 58% (**Figure21a**). The observed heel-to-toe bias is a common phenomenon observed in unconventional, lateral wells that occurs due to physical limitations of effectively pumping frac fluid to the toes of the wells. However, for this study, the observed heel-to-toe bias may be exaggerated due to the heel stages being alternated between XLE and standard completion, while toe-ward only standard completion was used. This appears to be independent of the geologic zone in which the wellbore was drilled, as even within the Laminated MB2, the heel-ward stages (38-40) have significantly higher cluster efficiencies than the

more toe-ward stages (32-36) (**Figure 21a**). 'It's also evident from this figure that the higher cluster count XLE stages (38, 40, 42, 44, 46, and 48) typically have higher cluster efficiency than those interspersed 8 cluster stages (39,41, 43, 45, 47), as previously discussed.

For SC-H3 (MB), cluster efficiencies for each geologic zone range from 75% to 85% **(Figure 22a)**. Cluster initiated in the Massive MB2 appears to have a slightly lower efficiency. Because of the strong overprint of the heel-to-toe bias, it is not definitive that lithologic differences in the rocks control the slight decrease in cluster efficiency in this zone. The heel-to-toe bias leads to over half of the sampled clusters initiated in the Massive MB2 to fall toward the toe of the well, bringing down the overall efficiency of clusters initiated in this geologic zone.

Similar to the SC-DSU H-3 (MB), the SC-H2 (TF) shows a robust heel-to-toe bias in cluster efficiency with heel clusters having an average cluster efficiency of 96% and toe-ward cluster having an average cluster efficiency of 69% (**Figure 21b**). Overprinted on the observed heel-to-toe bias, is a heel-to-toe transition from the wellbore being dominantly in the TF1 Mudstone and TF1 Basal Clean at the heel, to the toe being drilled predominantly in the more interbedded TF1 Interbedded. Based on the commonly observed heel-to-toe bias in cluster efficiency (not just in this study) due to limitations of physical transport of proppant to the toe of lateral wells, we are interpreting the observed heel-to-toe bias on the SC-DSU H-2 (TF) to be caused by general cluster efficiency degradation and not an effect of geologic zone transition.

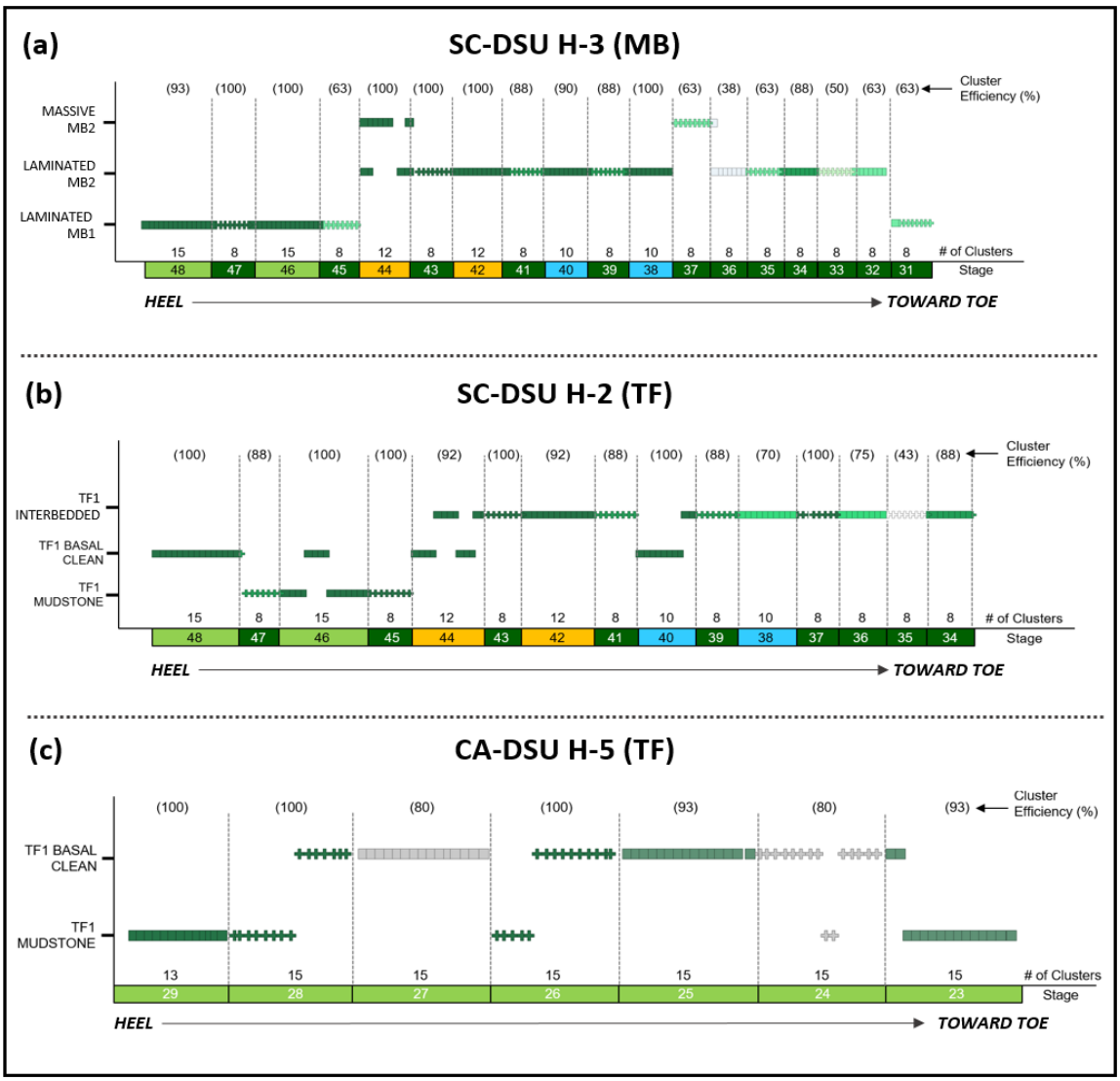

Figure 21: This figure illustrates, the trajectory of the lateral portion of (a) SC-DSU H-3 (MB), (b) SC-DSU H-2 (TF), (c) CA-DSU H-5 (TF) wellbores. The y-axis displays the geologic zone categories, in stratigraphic order from top to bottom for each well. The x-axis is measured depth along the wellbore, heels are to the left, and the toe-ward portion of the wells are to the right. Each symbol (plus or square) represent an individual cluster, grouped into stages by the vertical dashed grey lines. The pluses and squares have no significance other than to draw the eye to stage changes. The symbols are colored by cluster efficiency (darker green = greater efficiency; lighter green = medium efficiency; grey = low efficiency). Stage number and the number of clusters per stage are labeled across the bottom of each inset. Stage numbers are color coordinated based on the number of clusters per stage. Cluster efficiency (%) is labeled across the top of each inset.

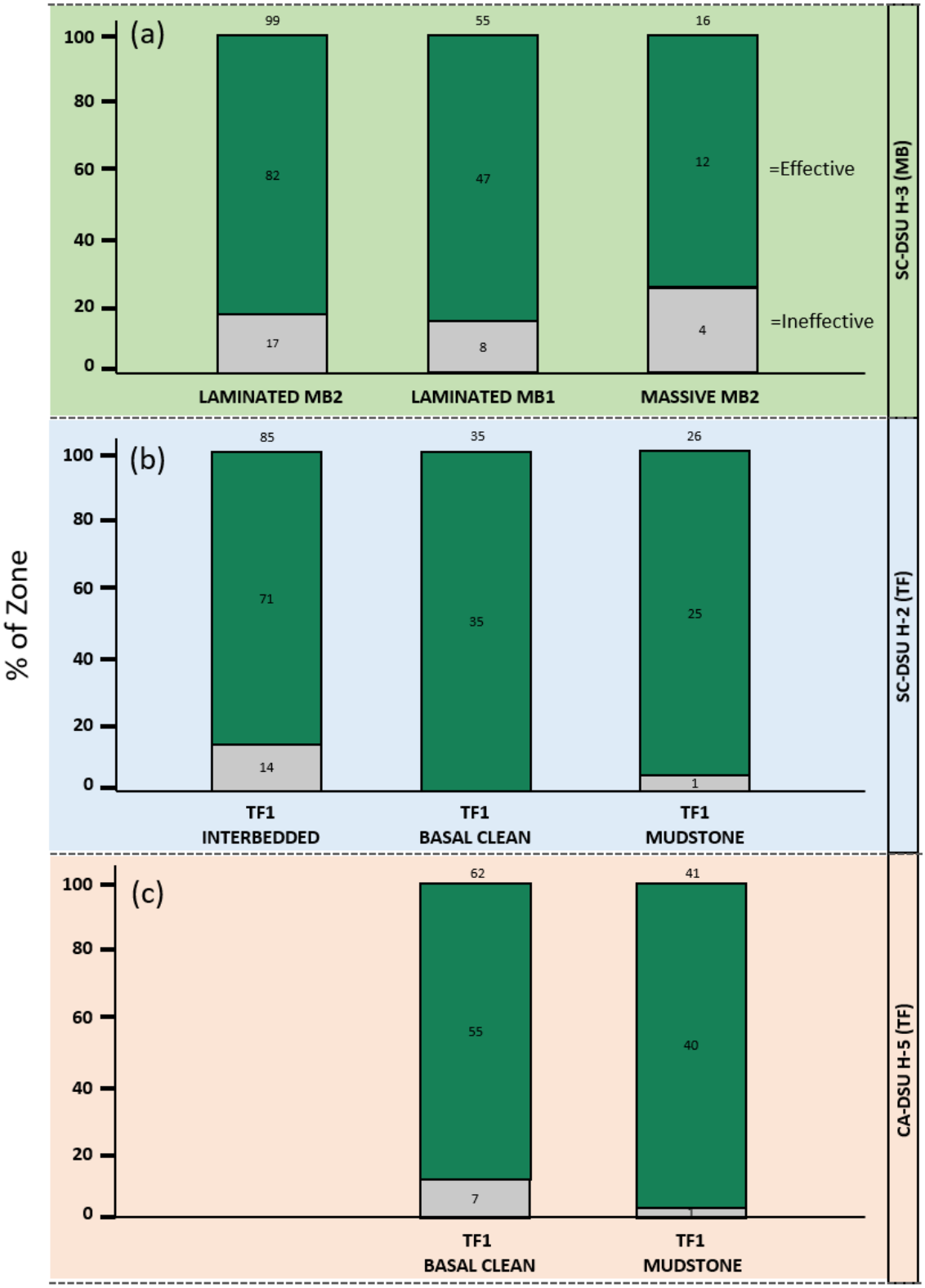

Figure 22: Bar graph showing the number of each clusters within each geologic zone that were effective (dark green), and ineffective (grey) for (a) SC-DSU H-3, (b) SC-DSU H-2, and (c) CA-DSU H-5. The y-axis shows the percentage of effective and ineffective clusters compared to the total number of clusters within each geologic zone. See text for more a detailed explanation.

To summarize the results of SC-DSU H-2 (TF), the cluster efficiencies range from 84 % to 100% **(Figure 22b)**. The cluster efficiencies for the TF1 Basal Clean and the TF1 Mudstone are, within uncertainty, identical. However, clusters that initiated in the TF1 have overall lower efficiency compared to the other two zones. It's unclear whether the observed reduced cluster efficiency for TF1 Interbedded initiated clusters is controlled by the difference in the nature of the geologic zones (interbedded vs. not) or by the more considerable overprinted heel-to-toe bias that was previously discussed. It appears more heel-ward clusters that initiated in the TF1 Interbedded have higher cluster efficiencies (95%) than those in the toe (69%), indicating that the overprinted heel-to-toe bias is controlling the difference in cluster efficiency between the TF geologic zones. Therefore, there doesn't seem to be a clear, significant difference in the cluster efficiency between the clusters initiated in each of the TF zones/facies.

Well CA-H5 (TF) cluster efficiency by stage is shown in **Figure 21c.** Note that there are significantly less number of stages sensed on this well (7) than on the SC-DSU wells (~15). This is due to all the heel-ward stages of the CA-DSU H-5 (TF) being high cluster count stages, which results in physically longer stages, as opposed to the SC-DSU, which had alternating high cluster count and low cluster count stages (**Figure 21a, b, c**). As opposed to the SC-DSU wells, the CA-DSU H-5 (TF) doesn't exhibit a clear heel-to-toe bias in cluster efficiency.

To summarize, cluster efficiencies for each geologic zone of the CA-DSU H-5 (TF) range from 89% to 98%. (**Figure 22c**). For this well, there doesn't seem to be a clear heel-to-toe bias across the sensed stages; therefore, the difference in cluster efficiency between the TF1 Mudstone and the TF1 Basal Clean may be geologically controlled. Conceptually, this is backward from our understanding of rock behavior. The muddier TF1 Mudstone unit has a lower 'Young's Modulus (~6.9) compared to the more clean, brittle TF1 Basal Clean (~7.6) in the CA-DSU area. However, there is a stark contrast in porosity and water saturation between these two units, with the TF1 Mudstone having lower porosity (4.7% vs. 5.1%), but drastically higher water saturation (98% vs. 52%) (**Table 2**). Perhaps the higher calculated cluster efficiency for the TF1 Mudstone is related to higher flow volumes and rates of water from the highly water-saturated TF1 Mudstone, manifested as louder acoustic noise on the fiber DAS data. Previous studies have suggested that much of the water produced from MB and TF wells is coming from the Three Forks. These studies further explicitly suggested, that the water is coming from more muddy facies from within the TF (e.g., TF1 Mudstone) (**Wright et al., 2019**). Additional work should be done to investigate this hypothesis.

The results of this study indicate that geologic heterogeneity has no identifiable cluster efficiency in Bakken and Three Forks wells when using XLE. Slight differences in cluster efficiency are likely due to the general heel-to-toe bias and not due to the lithologic property variability between different geologic zones intersected by the wellbore. Based on the positive efficiency results from the fiber optics, tracers, and camera data collected in our pilot wells, the authors feel confident continuing with a geometric completion design for an economically optimum solution. Geometric completions combined with XLE allow for increased clusters per stage, which reduces operational complexity, time, and cost. The lack of correlation of cluster efficiency with geologic zone concluded in this study does not negate a potential link between cluster-level production rates/water cut with a geologic zone. This has been highlighted as an area for future research.

Conclusions

Using multidisciplinary analysis and obtaining different types of completions data allowed the operator to prove the XLE design and apply XLE to the standard design. The main conclusions from this project are the following:

1. eXtreme limited entry (XLE) design method is proven by multidisciplinary analysis to consistently indicate high cluster efficiency (average of more than 90%) and allow completions engineers to push the boundary of the number of clusters per stage.
2. There is a good agreement in diagnostic data results from RA tracer, deployable fiber optic, and downhole camera, indicating that high clusters efficiency in XLE stages. However, there is less agreement between perforation erosional data and cluster productivity data from fiber-optic. Additional study is required to understand the relationship between erosion data and cluster-level production.
3. XLE designs allow the engineers to extend completion stage length without a reduction in the efficiency of fluid injectivity in each cluster. This technique was able to reduce between 4-12 stimulation stages based on the original design of the trial wells in this paper. The operator was able to save approximately 10% of the original well completion cost.
4. The majority of the XLE stages (70%) show heel to toe bias to some degree based on downhole camera perforation data.
5. Downhole camera can indicate the injection of proppant by erosion on perforations, but the erosion data cannot be directly correlated to cluster-level production. Additional studies need to be performed to understand the correlation between erosion and the volume of proppant injected.
6. The most eroded perforation holes are on the low side of the well, indicating that gravity is affecting proppant distribution and flow in the wellbore.
7. Quality control of perforating is critical to ensure accurate and consistent EHD, phasing, cluster spacing, and, most importantly, XLE pressure. Variations in EHD and unplanned perforation hole can result in reduced cluster efficiency, with larger perforations taking more fluid and eroding much faster
8. Step down tests are a good and cost-effective technique to evaluate XLE strategies, providing measurements of limited entry pressure and percentage of open perforations.
9. RA tracer and fiber optic data show that if the designed limited entry pressure is reached, high clusters efficiency is also achieved.
10. Using XLE design as described in this paper results in good completions efficiency despite geologic heterogeneity found in the Bakken.
11. Plug leakage issues can be captured by RA tracer data and can significantly affect the stimulation fluid distribution in the stage.

Acknowledgment

The authors wish to thank Hess Corporation and the Bakken Team for permission to publish this work. Special thanks to Matthew Lawrence with Ziebel for his contribution in the deployable fiber work section,

Christian Gradl for his early involvement and support in the project, Swathika Jayakumar with Core laboratories for RA tracer analysis, Mark Wiltosz, and Jeff Whitaker with EV camera for downhole camera imaging analysis.

References

Ahmed Attia, Ziebel; Jared Brady, Devon Energy; Matthew Lawrence and Robert Porter. Validating Refrac Effectiveness with Carbon Rod Conveyed Distributed Fiber Optics in the Barnett Shale for Devon Energy. SPE-194338

Ashton, T., Ly, C.V., Spence, G. and Oliver, G. (2013). Portable technology puts real-time automated mineralogy on the well site. SPE URC, Extended Abstract

Cramer, D., Friehauf, K. , Roberts, G., Whittaker, J. (2019, February 5) Integrating DAS, Treatment Pressure Analysis and Video-Based Perforation Imaging to evaluate Limited Entry treatment Effectiveness. SPE 194334-MS

Far, M.E., Buller, D., Quirein, J., Gu, M. and Gokaraju, D. (2015). A new integrated data analysis algorithm and workflow for optimizing horizontal well completion in unconventional reservoirs. SPWLA 56th, Annual Logging Symposium, Expanded Abstracts

Ganguly, U. and Cipolla, C. (2012). Multidomain data and modeling unlock unconventional reservoir challenges. JPT Technology Update, 32-37

Hogancamp, N., Pocknall, D. (2018). The biostratigraphy of the Bakken Formation: A review and new data. Stratigraphy. DOI: 10.29041/strat.15.3.197-224

Miller, C., Waters, G. and Rylander, E. (2011). Evaluation of production log data from horizontal wells drilled in organic shales. SPE North American Unconventional Gas Conference and Exhibition, The Woodlands, Texas, USA.

Murphree, C., Kintzing, M., Robinson, S., Sepheri, J., Evaluating Limited Entry Perforating & Diverter Completion Techniques with Ultrasonic Perforation Imaging & Fiber Optic DTS Warmbacks. SPE-199712-MS

Pilcher, R.S., Coisek, J.M., McArthur, K., Homan, J. and Schmitz, P.J. 2009. Ranking production potential based on key geological drivers—Bakken case study. Paper presented in International 423 Petroleum Technology Conference, Bangkok, Thailand, February 7-9, 2009. 424 http://dx.doi.org/10.2523/IPTC-14733-MS

Senters, C. W., Warren, M. N., Squires, C. L., Woodroof, R. A., & Leonard, R. S. (2015, September 28). Reducing Costs and Optimizing Drilling and Completion Efficiencies in Unconventional Plays Using Completion Diagnostics. Society of Petroleum Engineers. DOI: 10.2118/174844-MS.

Sonnenberg, S., Pramudito, A. (September 2009). Petroleum geology of the giant Elm Coulee field, Williston Basin. AAPG Bulletin. DOI:10.1306/05280909006

Swami, V., Spence G., Gentilhomme, T., Bachman, B., Letizia, M. and Lipp, C. (2017). From geology to production: a completion optimization case study from Cleveland Sand, Oklahoma. CGG Special Topic: Unconventionals and Carbon Capture and Storage, 83-92.

Weddle, P., Griffin, L, and Pearson, M (2018, January 25). Mining the Bakken II- Pushing the Envelope with EXtreme Limited Entry Perforating. SPE-189880-MS

Woodroof, R.A., Asadi, M., Warren, M. N. "Monitoring Fracturing Fluid Flowback and Optimizing Fluid Cleanup Using Frac Tracers", Paper SPE 82221, presented at 2003 SPE European Formation Damage Conference, The Hague, The Netherlands, 13-14 May.

Wright, C.A.: "On-Site Step-Down Test Analysis Diagnoses Problems and Improves Fracture Treatment Success," Hart's Petroleum Engineer International (1997).

Wright, S., Franks, S., Pantano, J., Kloska, M., Wolters, J. (2019). Understanding Dynamic Production Contribution from Hydraulically Fractured Middle Bakken and Three Forks Wells in the Williston Basin, ND Using Time-Lapse Geochemistry. URTeC. DOI: 10.15530/URTEC-2019-142

Nomenclature

Bbl = *Barrel*

BPM = *Barrels per minute*

DSU = *Drilling Spacing Unit*

DAS = *Distributed Acoustic Sensing*

DTS = *Distributed Temperature Sensing*

EC = *Enhanced Collapse*

EHD = *Entry Hole Diameter*

Gpt = *gallon per thousand*

LBS = *Lower Bakken Shale*

ISIP = *Instantaneous Shut-In Pressure*

MB = *Middle Bakken*

nd = *Narno darcy*

Psi = *Pound per square inches*

P&P = *Plug and perf*

PCE = *Perforation Cluster Efficiency*

POOH = *Pull Out of Hole*

RA = *Radio Active*

SPF = *shots per foot*

TVD = *True Vertical Depth*

TF = *Three forks*

UBS = *Upper Bakken Shale*

XLE = *eXtreme Limited Entry*